Behavior of uranium 5*f* states in a graphite intercalation compound

S. Danzenbächer, S. L. Molodtsov,* J. Boysen, and C. Laubschat
Institut für Oberflächenphysik und Mikrostrukturphysik, TU Dresden, D-01062 Dresden, Germany

A. M. Shikin and S. A. Gorovikov
Institute of Physics, St. Petersburg State University, 198904 St. Petersburg, Russia

Manuel Richter
Department of Theoretical Solid State Physics, IFW Dresden, D-01171 Dresden, Germany
(Received 29 August 2000; revised manuscript received 11 January 2001; published 15 June 2001)

We present an angle-resolved photoemission (PE) and angle-resolved resonant PE study of a single crystalline U-graphite intercalation compound (U-GIC). Stage-2 U-GIC samples were prepared *in situ*, by deposition of U metal onto clean graphite (0001) substrates and subsequent annealing. As follows from comparison with the results of local-density approximation (LDA)-linear combination of atomic orbitals (LCAO) band-structure calculations, the electronic structure of the grown GIC may be understood by the filling of unoccupied graphite π_0^* bands by additional electrons contributed by U. This charge transfer is monitored by a shift to higher binding energies of all graphite-derived PE features and the appearance of an additional rather narrow feature at the Fermi energy (E_F), upon intercalation. This Fermi-level peak is superimposed by a sharp U 5*f* signal, that is located directly at E_F and reveals no trace of multiplet splitting or dispersion. Results of band-structure calculations indicate a weak hybridization of the U 5*f* states and their occupation of about 2. A description of the observed 5*f*-related spectra in the framework of a single-impurity Anderson model is possible.

DOI: 10.1103/PhysRevB.64.035404 PACS number(s): 79.60.−i, 68.65.−k, 73.21.−b, 71.28.+d

I. INTRODUCTION

The physical and chemical properties of actinide systems are mainly determined by the behavior of the actinide 5*f* orbitals that ranges from ''atomiclike'' to ''bandlike,'' depending on the surrounding atomic arrangement. Due to a node in the radial wave function, the 5*f* states are spatially more extended than the 4*f* states in lanthanides and are, therefore, subject to stronger *f*-*f* and *f*-valence states hybridization. As a consequence, the 5*f* states behave bandlike in *hcp* U metal as it has been shown recently by probing their energy dispersion by means of angle-resolved photoemission (PE).[1,2] In the pure metal, the bandlike properties of the U 5*f* states stem from direct *f*-*f* interaction rather than from *f*-*d* hybridization and a description in the framework of single-particle band-structure calculations is possible.[1] Among the other elemental actinide metals, the 5*f* states are expected to take part in chemical bonding only up to Np, while starting with Am, they are predicted to be localized. Pu seems to be a borderline case.[3] In actinide compounds the situation is more complicated. Due to the increased interatomic distance to the nearest actinide neighbors, already in some U compounds the 5*f* states reveal correlation-related properties such as magnetic phenomena, mixed valency, heavy fermion, and superconducting behavior.[4] Therefore, investigations of U systems are of high interest for fundamental research.

Among other U systems, U-graphite intercalation compounds (GIC's) seem to be promising candidates to study the interplay between 5*f* hybridization and localization phenomena. GIC's consist of stacks of graphite sheets (graphenes), which alternate with ordered two-dimensional (2D) intercalant layers.[5] Hereby, intercalated atoms are located between the centers of two C hexagons of neighboring carbon layers. Due to this arrangement, the *A*-*B*-*A*-*B* stacking sequence of the graphite layers is changed into an *A*-*A* sequence around the intercalant layer, and the GIC's reveal a $(\sqrt{3}\times\sqrt{3})R30°$ or 2×2 overstructure with respect to the (0001) plane of pristine graphite. In these structures, the nearest-neighbor distances between intercalant atoms are considerably larger than in the corresponding elemental solids [Fig. 1(a)]. Hence, contrary to U metal, the 5*f* states in U-GIC may be expected to be rather localized due to a negligible overlap between 5*f* orbitals of neighboring U atoms [Fig. 1(b)]. Since the atomic

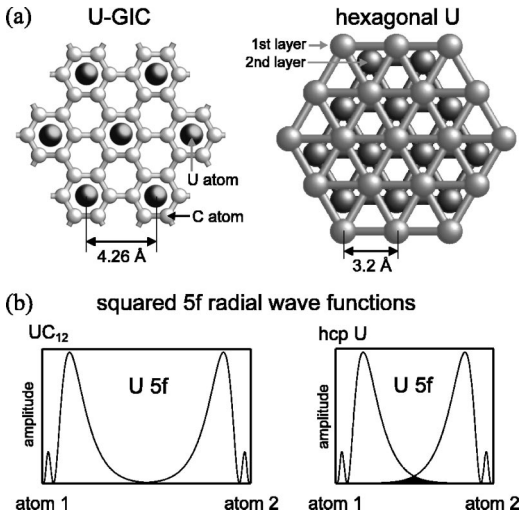

FIG. 1. (a) Crystalline structure of U-GIC and *hcp* U metal (top view). (b) Overlap of U 5*f* squared radial wave functions multiplied by r^2 of U-GIC (UC_{12}) and *hcp* U (shadowed area) for neighboring U atoms.

positions of the intercalant atoms are well defined, the opportunity to obtain well-ordered magnetic multilayer structures in U-GIC's arises, if the $5f$ states reveal atomiclike behavior.

Although in the recent past, GIC's of different metals have been subject of numerous experimental and theoretical studies due to their interesting two-dimensional structural, electronic, and transport properties,[5] no attempts for *in situ* intercalation of actinides (except our earlier studies)[6,7] were reported. It was shown that particularly alkali-GIC's can easily be grown *in situ* under ultrahigh-vacuum (UHV) conditions. Other metals, which are characterized by more complex valence-band structures, including *d* and *f* states (e.g., transition metals, lanthanides, and actinides) make the intercalation process more difficult. Nevertheless it was shown[8–17] that deposition of lanthanides onto the (0001) surface of graphite followed by thermal annealing at certain temperatures leads to formation of surface compounds with electronic and crystalline structures similar to those of alkali-derived GIC's. Eu- and Yb-graphite systems are formed by direct diffusion of divalent rare-earth (RE) ions into the interlayer spacings of graphite[12,13] and may be considered as conventional bulk GIC's. On the other hand, graphite systems with trivalent RE's (La, Gd, and Tb), which were synthesized via a stage of RE-carbide formation, can be described as a thin layer of intercalationlike compound grown on the top of the (111) surface of RE dicarbide.[8,10,11,14–17]

In the present paper we report on an angle-resolved PE and resonant PE study of the electronic structure of graphite intercalated *in situ* with uranium. The samples were prepared under UHV conditions by deposition of U metal onto a clean graphite (0001) surface and subsequent annealing. The PE data are compared with results of band-structure calculations. It is found that the intercalation leads to a shift of all graphite-derived PE structures toward higher binding energies (BE's) and to the appearance of an additional narrow feature at the Fermi energy (E_F). This Fermi-level peak is superimposed by a sharp U $5f$ signal that is located directly at E_F and reveals no trace of multiplet splitting or dispersion. Since the band-structure calculations give evidence for only weakly hybridized character of the U $5f$ states and their occupation of about 2, a description of the PE data in the framework of a single-impurity (SI) Anderson model is proposed.

II. EXPERIMENTAL DETAILS

Single-crystalline flakes of natural graphite with typical diameters of 7–9 mm were cleaved with an adhesive tape and subsequently carefully degassed *in situ* during several hours at a temperature of 1700 K under UHV conditions. This procedure results in a clean surface, which reveals hexagonal low-energy electron diffraction (LEED) pattern characteristic of graphite (0001). Similar to the previous studies of GIC's,[6–17] *in situ* intercalation of U into the graphite matrix was achieved by thermal deposition of relatively thick layers of the intercalant (100 Å) onto the clean graphite surface followed by a step-by-step annealing. The deposition of U was performed at rates of 3–5 Å/min by means of electron bombardment of an U-metal filled tungsten crucible with a pin hole, which was heated up to temperatures of about 2300 K. The thickness of the deposited U films was monitored by quartz microbalances. The vacuum during evaporation was in the 10^{-10}-mbar range. Deposition at room temperature resulted in nonordered interfaces terminated by pure U-metal layers. Several stages of a step-by-step annealing (from 600 K to 1100 K) of the obtained U-graphite system led to a recovering of a periodic crystalline structure with a sharp GIC-like $(\sqrt{3}\times\sqrt{3})R30°$ reconstruction of the LEED pattern relative to that of pristine graphite (Fig. 2). No hint of a formation of carbidelike chemical compounds accompanied by a destruction of the graphite matrix as in the case of La(Gd, Tb) graphite interfaces,[8–11,14–17] could be observed during the annealing process. This indicates that, in contrast to the above trivalent RE's, U can be directly incorporated into graphite crystals.

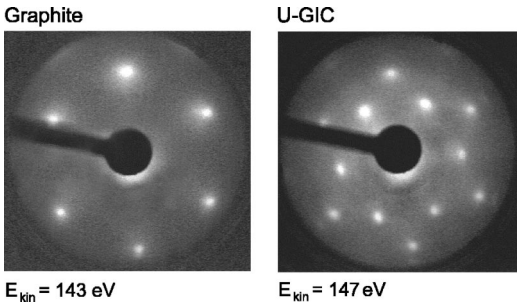

FIG. 2. LEED pattern of graphite and U-graphite compound.

The observed $(\sqrt{3}\times\sqrt{3})R30°$ reconstruction of the LEED image that is in accordance with crystalline structure of bulk RE-GIC's synthesized by a classic vapor-phase intercalation[18,19] points to a UC_6 surface stoichiometry for the samples grown in the present study. Note, however, that an estimation of the bulk composition, i.e., the stage of intercalation defined by the number of carbon planes laying between neighboring U layers, is not possible from the LEED experiment. The obtained sharp reconstructed LEED pattern did not change throughout several hours of data acquisition pointing to a chemically inert surface. This fact is related to the layered structure of the GIC, where U atoms are incorporated into the graphite matrix and the surface is formed by a carbon layer.

The measurements were performed at the Berliner Elektronenspeicherring für Synchrotronstrahlung (BESSY I) using radiation from the plane-grating-monochromator beamline SX/700 II. Angle-resolved valence-band photoemission spectra and resonant photoemission spectra at the U $5d \rightarrow 5f$ excitation threshold were taken with a hemispherical electron energy analyzer (ARIES, Vacuum Science Workshop, Ltd.) tuned to an energy resolution of 150 meV (full width at half maximum) and an angle resolution of 1°. The experiments were carried out at room temperature. In order to monitor graphite-derived bands of both π and σ symmetries, the photon incidence angle was selected to be 35° relative to the sample surfaces. The basic pressure during the measurements was always better than 1×10^{-10} mbar.

III. DETAILS OF THEORETICAL CALCULATIONS

Band-structure calculations for different sequences of U and graphene layers were carried out in the framework of the

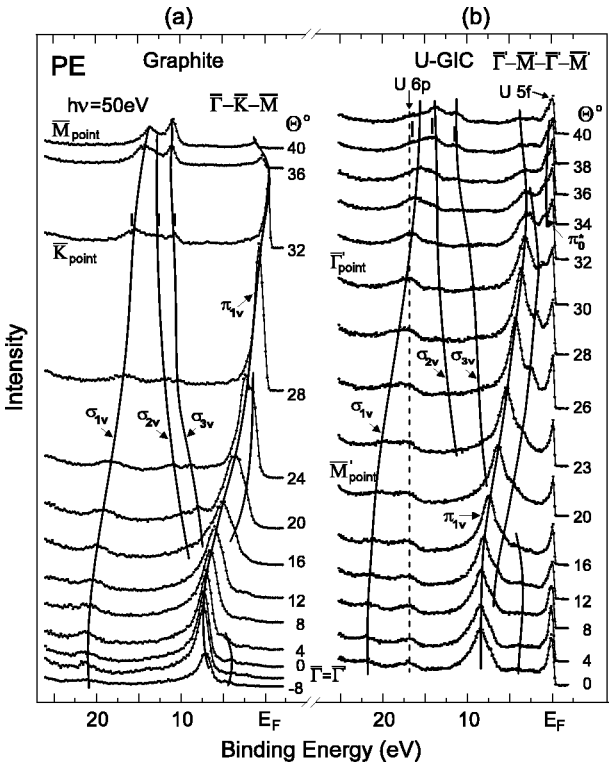

FIG. 3. EDC's of (a) graphite and (b) U-graphite compound measured at various Θ values along the $\bar{\Gamma}$-$\bar{K}$-$\bar{M}$ direction in the surface BZ of graphite and the $\bar{\Gamma}'$-$\bar{M}'$-$\bar{\Gamma}'$-$\bar{M}'$ direction in the BZ of U-graphite compound.

local-density approximation (LDA) using the Hedin-Lundqvist exchange-correlation potential.[20] A number of different stackings was considered since the correct layer sequence could not be directly extracted from the available experimental data. The U-GIC was treated as an ideal crystalline structure: no account was taken of surface and real structure effects. We employed the method of an optimized linear combination of atomic orbitals (LCAO)[21] in its fully relativistic version.[22] The set of atomic orbitals included the U 7s, 6p, 6d, and 5f states as well as the C 2s and 2p states. Since a transition from bandlike to localized behavior of the 5f states may be expected in U-GIC, we assumed also localized 5f configurations in our calculations. The localized behavior was simulated by treating the 5f's as core states.

IV. EXPERIMENTAL RESULTS

Two sets of angle-resolved energy distribution curves (EDC's), measured for pristine graphite and a U-graphite system after annealing to 1100 K, are shown in Figs. 3(a) and 3(b), respectively. The spectra were taken at 50 eV photon energy at various polar angles (Θ) along the $\bar{\Gamma}$-$\bar{K}$ direction in the first surface Brillouin zone (BZ) and the $\bar{K}$-$\bar{M}$ direction in the second surface BZ of graphite. For the grown U-graphite compound, this corresponds to a scan along the $\bar{\Gamma}'$-$\bar{M}'$-$\bar{\Gamma}'$-$\bar{M}'$ direction in the reconstructed surface BZ's as follows from the observed $(\sqrt{3}\times\sqrt{3})R30°$ overstructure of the LEED pattern. The spectra are normalized to the flux of the incident photons. The experimental band dispersions are guided in the figure by solid lines through the peak maxima.

In accordance with the results of earlier studies,[12,23–25] EDC's measured for graphite are characterized by four main photoemission bands. The π_{1v}-symmetry band originating from the C 2p_z orbitals disperses toward the Fermi level in the first Brillouin zone ($0°<\Theta<32°$). It reaches E_F close to the $\bar{K}$ point that is the only region in the BZ of graphite with finite density-of-states at the Fermi level. At larger polar angles this band shifts back toward higher BE's. At $\Theta<32°$, the π_{1v}-symmetry band reveals a high PE intensity. The PE weight of this band considerably decreases in the second BZ. The latter can be explained by Brillouin zone selection rules based on the interference of outgoing photoelectron waves from the two carbon atoms in the unit cell of graphene on their way to the detector.[26] The other three low intensity bands reveal σ symmetry. Two of them are degenerated at the $\bar{\Gamma}$ point. These bands, which have 2$p_{x,y}$ angular momentum character, disperse in the direction of higher BE's on the way from the center of the Brillouin zone to its border. They cross the π_{1v} band in the region of $\Theta\cong 8°$. For polar angles $\Theta>12°$ these bands are energetically split into two components marked by σ_{2v} and σ_{3v} in the figure. In the region of the border of the BZ, the 2$p_{x,y}$-derived bands overlap the 2s-originating band (σ_{1v} symmetry) giving rise to sp^2 hybridization characteristic for the hexagonally arranged graphite layers. According to the selection rules mentioned above[26] the PE intensities of all three σ symmetry bands grow in the second BZ.

The EDC's shown in Fig. 3(b) for each particular Θ, are similar to the corresponding PE spectra of pure graphite for BE's larger than about 2 eV. All graphite derived bands, presented in Fig. 3(a) are reproduced in Fig. 3(b). In the latter figure, however, these bands are shifted by up to 2.6 eV toward higher BE's depending on their symmetry and the point monitored in the BZ of the synthesized compound. The triplet structure observed in the region of the sp^2 hybrid bonds in pristine graphite (marked by vertical bars in the figure) is preserved in the U-graphite system. Characteristic variations of intensities of the π- and σ-originating features across the border of the Brillouin zone[26] indicate also, that the structure of graphenes is retained in the synthesized compound. Note that the above intensity variations are less pronounced than those in the case of pristine graphite. The PE signal related to the U 6p states is seen at about 17 eV BE. The important difference between EDC's shown in Figs. 3(a) and 3(b) is, however, a new intense peak that is located directly at E_F in the U-graphite system. A similar feature was observed for all alkali and RE-GIG's[8–10,12,16,17,27,28] studied up to now. In contrast to the mentioned intercalation compounds, in the U-graphite system, this Fermi-level structure is present for all polar angles of analyzing (not only in the region of the $\bar{K}$ point); its intensity is not strongly modulated with the change of Θ.

An important difference between pristine graphite and the synthesized U-graphite compound relates to the pronounced 2D character of the electronic structure of the compound, while some bands of graphite reveal rather strong dispersion

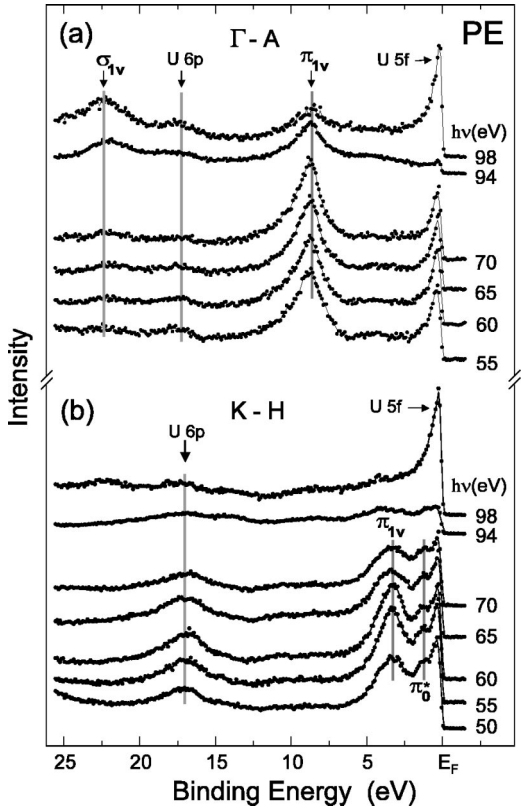

FIG. 4. PE spectra of the synthesized U-graphite compound measured with different hν along (a) the Γ-A and (b) the K-H high symmetry directions in the BZ of graphite.

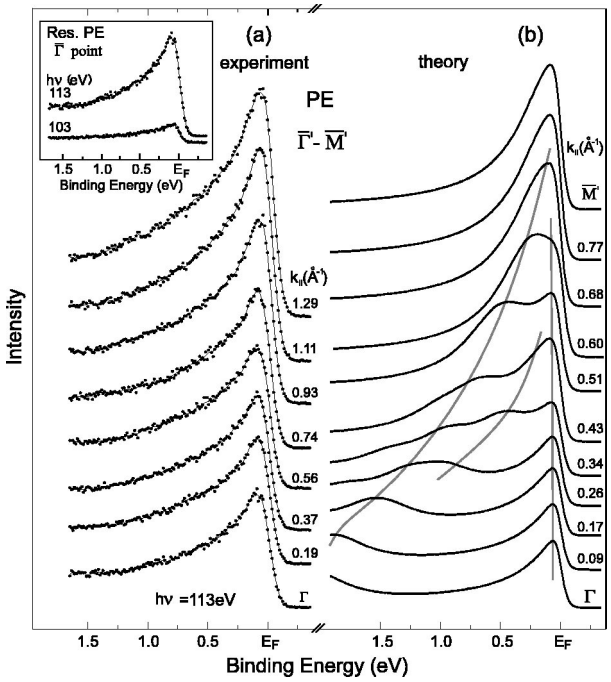

FIG. 5. (a) Resonant PE spectra taken along the $\bar{\Gamma}'$-$\bar{M}'$ direction. The inset shows a comparison of on- (hν=113 eV) and off-resonance (hν=103 eV) data for the Γ point. (b) Spectra simulated on the basis of the band-structure calculations.

in the direction perpendicular to the surface.[29] Two series of PE spectra of the grown U compound measured along the Γ-A and K-H high-symmetry directions in the BZ of graphite are shown in Figs. 4(a) and 4(b), respectively. As it is clearly seen, neither σ- nor π-symmetry graphite-derived features, as well as the peak at E_F, show BE variations when the energy of photon excitation is changed.

In RE-GIC's the structure at the Fermi energy was assigned mainly to the π_0^*-derived unoccupied bands of graphite,[8,9,12,16] which become filled in the intercalation compounds due to valence electrons supplied by the RE atoms. The π_0^* bands sink below E_F close to the border of the BZ of graphite, while in the inner part of the BZ they are still located above the Fermi energy. The remarkably different behavior of the Fermi-energy peak in Fig. 3(b) suggests an alternative nature of this PE signal. It could be assigned to U $5f$ electronic states, which are located in the region of E_F and characterized by a high cross section of photoexcitation for the photon energy used. This supposition is in accordance with a characteristic suppression of the $5f$-derived signal for U systems at hν=94 eV followed by its strong enhancement at hν=98 eV (Refs. 30–32) that is observed also for the Fermi-energy feature in Fig. 4.

To identify $5f$-derived photoemission features within the valence bands of the U-graphite system, resonant photoemission at the U $5d \rightarrow 5f$ excitation threshold was applied. In the present case the resonant PE is based on a Fano-type interference[33] between direct photoionization of a $5f$ state ($5f^n \rightarrow 5f^{n-1}+e^-$) and photoexcitation of an U $5d$ electron into an unoccupied $5f$ state ($5d^{10}5f^n \rightarrow 5d^9 5f^{n+1}$) followed by a participator decay ($5d^9 5f^{n+1} \rightarrow 5d^{10}5f^{n-1}+e^-$). By means of the resulting strong cross-section variation, the PE response of the U $5f$ states can be separated from non-f-derived emission from carbon and uranium. In our recent study of La metal[34] we showed that resonant PE in its angle-resolved mode allows us to determine the angular momentum character of valence-band electronic states across the BZ. We apply this method in the present experiment to analyze possible contributions of $5f$ states to Bloch states of the U-graphite compound along the $\bar{\Gamma}$-$\bar{M}'$ high-symmetry direction. Corresponding PE spectra are shown in Fig. 5(a). In all spectra the observed strong signal at E_F is due to $5f$ emissions as concluded from a comparison of on- (hν=113 eV) and off-resonance (hν=103 eV) data shown for the $\bar{\Gamma}$ point in the inset in Fig. 5. The $5f$ Fermi-energy peak reveals no fine structure or multiplet splitting. For all emission angles the maximum of the PE intensity is located at E_F within the instrumental resolution. No evidence for a $5f$ band dispersion can be found in the presented EDC's in contrast to the situation encountered in U metal.[1] This observation implies a description of the $5f$'s in the obtained compound beyond single-electron-band models.

V. DISCUSSION

The presented experimental results show that an U-graphite system with characteristics of an intercalation compound was grown in the present study. This conclusion

is based on the LEED pattern and the discussed similarities of the graphite-derived photoemission bands shown in Figs. 3(a) and 3(b). As seen from the experiment, the sp^2 hybrid bonds, which build hexagonal cells of graphenes, are present in the synthesized compound. Also the Brillouin-zone selection rules derived in Ref. 26 from the particular structure of the elementary unit cell of graphene, are reproduced in the U-graphite system. Similar to other GIC's,[8,9,12,35,36] no pronounced folded PE bands, according to the observed $(\sqrt{3}\times\sqrt{3})R30°$ overstructure of the LEED pattern, were observed. The nondispersive behavior of all valence-band structures observed along the Γ-A and K-H direction (Fig. 4) indicates an almost two-dimensional character of the crystalline arrangement and electronic structure of the samples.

As was observed for all other GIC's intercalated with donor species (e.g., alkalies or RE's), the π- and σ-symmetry bands in U-GIC are almost rigidly shifted toward higher BE's as compared to their positions in pristine graphite. As a general trend the observed energy shift in the U-GIC is, however, smaller than in the case of the RE-GIC's. Close to Γ point it amounts to only 1.1 eV for the π_{1v}-derived band, while it reaches about 1.6 eV for this band in the case of RE-GIC's.[8,9,12] This fact can be understood by the higher electronegativity of U as compared to that of alkalies and RE's (Ref. 37) that results in a weaker charge transfer from the intercalant to the carbon states.

In situ intercalation of U into single-crystalline graphite was achieved by a method cross proved in our previous studies of RE-GIC's.[6–17] In spite of the very high chemical reactivity of U (Refs. 3, 38) carbide formation is not observed as a precursor of intercalation as it is the case with all trivalent RE's (Refs. 8–10). Note, however, that the covalent radius of U (1.42 Å) is about 20% smaller than that of, e.g., La (1.69 Å).[39,40] Since intercalant atoms are located between centers of tightly bound carbon hexagons of neighboring graphenes, the distances between the outermost covalent orbitals of guest (i.e., U 6d or La 5d) and host atoms (C 2p) are much larger in the U-graphite system. The latter reduces covalent interaction leaving, nevertheless, the possibility of ionic bonding related to the different values of electronegativity; 1.4 for U and 2.5 for C, respectively.[37]

The observed for U-GIC $(\sqrt{3}\times\sqrt{3})R30°$ reconstruction of the crystalline structure of pristine graphite is similar to that obtained upon *in situ* intercalation of RE's. This type of lattice reconstruction was also found for bulk RE-GIC's synthesized by the classic vapor-phase intercalation.[18,19] In contrast to bulk intercalation, the *in situ* intercalation method applied here is restricted to incorporation of guest atoms within the first few graphite layers close to the surface. Although the $(\sqrt{3}\times\sqrt{3})R30°$ LEED image points to a local UC_6 stoichiometry, it is not easy to estimate the real bulk composition, i.e., the stage of intercalation. On the other hand, different stages of intercalation are related to a different number of donor electrons supplied by U per C atom. We have performed band-structure calculations for U-GIC's of different stages. The results of our analysis show, that for a hypothetical stage-1 compound (UC_6) no agreement with the measured EDC's can be obtained. However the calculated electronic structure of a stage-2 intercalation compound (UC_{12})

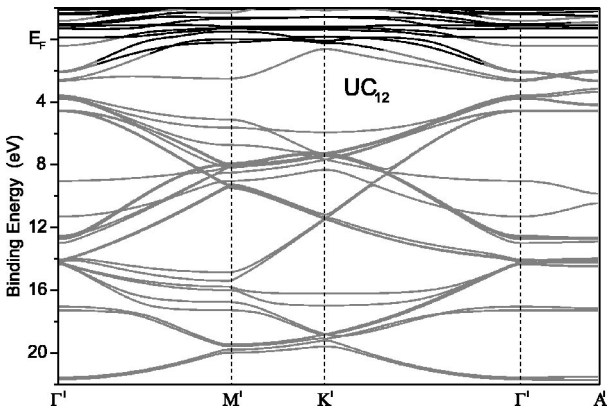

FIG. 6. Electronic bands, calculated for a bandlike U 5f configuration along the high-symmetry directions in the BZ of UC_{12}. Branches, which contain more than 20% of f angular momentum character, are shown by thick-solid lines.

is in good agreement with the experimental data. This fact indicates that a compound with [-U-C-C-] stacking sequence [as in the case of RE-GIC's (Ref. 12)] was likely synthesized in the present study.

In contrast to hcp U metal, where the 5f states reveal clear bandlike properties that arise from a direct overlap of the 5f orbitals of neighboring U atoms[1] (the hcp U-U nearest neighbor interatomic distance is 3.2 Å), in U-GIC no dispersion of the 5f's was observed [Fig. 5(a)]. According to Fig. 1(b), there is essentially no overlap between 5f orbitals in the intercalation compound, since the U-U interatomic distance amounts here to 4.26 Å. Alternatively, bandlike properties of the 5f states might be caused by their hybridization with C 2p states. We have investigated this possibility by performing LDA-LCAO band-structure calculations for UC_{12} including 5f states into the set of atomic valence orbitals. The calculations yield an overlap between 5f and π_0^* symmetry graphite-derived orbitals, which is only slightly stronger than that between 4f and π_0^* states in Eu-GIC, where the 4f states are found to be strongly localized.[12] The calculated bands along high-symmetry directions in the BZ of UC_{12} are shown in Fig. 6. Weak dispersion along the Γ'-A' direction is in agreement with the experimental results obtained in the normal emission PE experiment [Fig. 4(a)]. Branches, which contain more than 20% of f angular momentum character are shown by thick-solid lines in the figure. The obtained f-symmetry bands are rather narrow indicating a possible tendency to localized behavior. From the band-structure calculations a 5f occupation close to 2 is found pointing to a valency of U in this compound close to 4. Assuming that on-resonance PE spectra reflect only the 5f character of the wave function, model spectra may be generated extracting the corresponding information from the band-structure calculation. Figure 5(b) shows the results of such simulations, where peak positions correspond to the location of individual band and peak intensities reflect the squared 5f admixture to the wave functions. Taking into account finite lifetime and energy-resolution effects, a constant linewidth similar to that observed in the experiment was assumed. A clear dispersion of individual bands is visible in the simu-

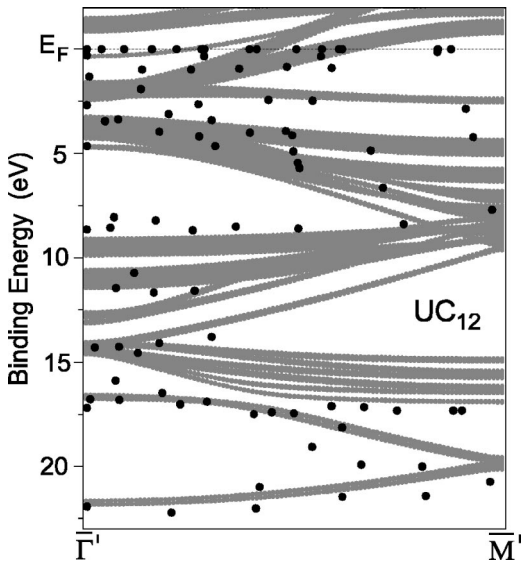

FIG. 7. Band structure of the stage-2 U-GIC (localized U $5f^2$ configuration), calculated within the Γ'-A'-L'-M' plane and projected onto the $\overline{\Gamma}'$-$\overline{M}'$ direction, in comparison to the measured band dispersions.

lated spectra, that, however, is not observed in the experimental spectra [Fig. 5(a)]. This fact can be taken as an additional indication for a localized character of the $5f$ electrons and, consequently, further calculations were performed with localized $5f$ configurations. It should be noted, however, that only dipole selection rules were considered in the simulated spectra, Fig. 5(b). Thus, quenching of the high binding-energy contributions due to crystal symmetry reasons cannot be ruled out.

In order to study the effect of U valency on the electronic structure of U-GIC, band-structure calculations for two localized configurations, $5f^2$ (tetravalent) and $5f^3$ (trivalent) were carried out. A good matching of the experimental data to theoretical bands was only achieved for the $5f^2$ configuration, while for a $5f^3$ configuration, strong deviations from experimentally observed band positions were obtained. Apart from the $5f$ states, only slight difference between bands, calculated for the localized $5f^2$ configuration and bandlike $5f$ states, is found. Figure 7 shows the band structure of the stage-2 U-GIC (localized U $5f^2$ configuration), calculated within the Γ'-A'-L'-M' plane and projected onto the $\overline{\Gamma}'$-$\overline{M}'$ direction in comparison to the measured band dispersions. Only pronounced experimental features are considered in this figure.

A localized character of the $5f$ states seems to be not consistent with the appearance of the $5f$ PE signal directly at the Fermi energy and the lack of multiplet splitting. Assuming, however, a scenario where a localized $5f^2$ ground state is almost degenerate with the $5f^1$ final state, the PE spectrum would consist of a pure $5f^1$ final state just at E_F. Since for actinides the $^2F_{5/2}$ component of this final state is predicted to be weak, in fact no significant multiplet structure is expected. The situation becomes complicated by consideration of hybridization that will lead to finite admixtures of other $5f^n$ configurations to the $5f^2$ ground state and, consequently, to the appearance of different $5f^{n-1}$ final-state multiplets in the PE spectra. Quantitatively this situation may be described by an extension of the simple single-impurity Anderson model presented by Imer and Wuilloud.[41] Here, the valence band is approximated by a single level at E_F. ϵ_f denotes the energy of a bare $5f^1$ state, the hybridization parameter Δ describes the hopping between $5f$ and valence-band states and U_{ff} represents the on-site Coulomb repulsion energy of two $5f$ electrons. This model that has been applied successfully to the $4f$ states of Ce systems may also be applied to U $5f$ electrons if in addition to f^0, f^1, and f^2 configurations present in Ce systems, the existence of a f^3 configuration is also considered. The configuration mixing of the ground state is then derived from the diagonalization of the model Hamiltonian

$$H=\begin{bmatrix} 0 & \Delta & 0 & 0 \\ \Delta & \epsilon_f & \sqrt{2}\Delta & 0 \\ 0 & \sqrt{2}\Delta & 2\epsilon_f+U_{ff} & \sqrt{3}\Delta \\ 0 & 0 & \sqrt{3}\Delta & 3\epsilon_f+3U_{ff} \end{bmatrix} \tag{1}$$

and the $5f$ PE spectrum is obtained by a projection of the ground state onto the individual excited states by means of the transition operator. For $\Delta=0$, the assumption of a $5f^2$ ground state demands $2\epsilon_f+U_{ff}<\epsilon_f$ [corresponding to $E(5f^2)<E(5f^1)$] and $2\epsilon_f+U_{ff}<3\epsilon_f+3U_{ff}$ [corresponding to $E(5f^2)<E(5f^3)$]. These conditions can be fulfilled with $\epsilon_f=-U_{ff}-\delta$, where δ denotes the observed $5f^1$ binding energy in the PE spectrum. In the present case, δ must be assumed to be smaller than 0.2 eV in order to yield a consistent description of the spectra. The magnitude of U_{ff} is more difficult to estimate. In $4f$ systems, U_{ff} amounts to ~8 eV, the corresponding d-d interaction energy in Ni amounts to 6 eV. For uranium, U_{ff} values around 2–3 eV are discussed.[42–44] In the present case, the actual value of U_{ff} is of secondary importance since it defines only the binding energies of $5f^0$ and $5f^3$ final states. An important point is, however, that U_{ff} is much larger than δ. In this case, finite values of Δ lead essentially to $5f^1$ admixtures to the ground state. Calculated model spectra, where the individual final states are described by simple Lorentians, are shown in Fig. 8. For finite values of Δ, $5f^0$ and $5f^2$ final states appear in addition to the prominent $5f^1$ final state at $\sim -U_{ff}$ and 0 eV binding energy, respectively. On the left panel of Fig. 8, this effect is illustrated for constant Δ, U_{ff}, and different values of δ. As it is evident from the figure, δ must be positive and larger than Δ to avoid strong $5f^0$ emissions in the spectra. The right-hand side of Fig. 8 shows the interplay of δ and Δ in more details. Here, also the $5f^2$ component is shown and the actual $5f$ occupancies n_f of the individual excited states are given. Note, that n_f of the $5f^2$ component is identical to that of the ground state. The fact, that in the real spectra no $5f^0$ emission is observed in the region between 1 and 5 eV binding energies, restricts Δ to small values. One should consider, however, that the signal of a $5f^0$ peak might be washed out by lifetime broadening. In Ce metal the width of the $4f^0$ peak is about 10 times larger than that of the $4f^1$ emission, and similar situations are observed for the lower

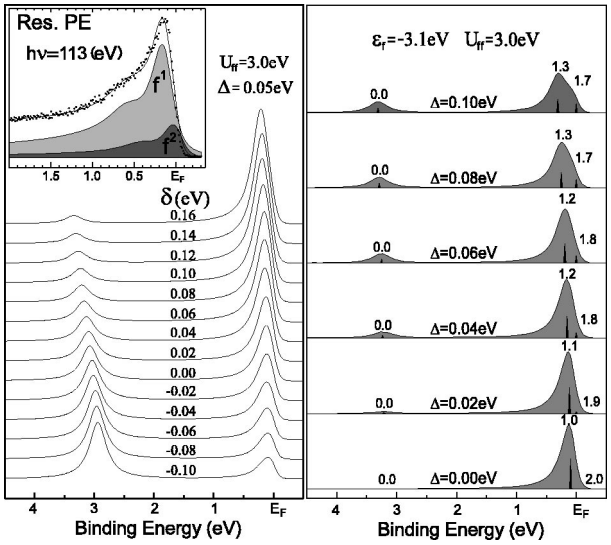

FIG. 8. Calculated PE spectra simulated on the basis of a single-impurity Anderson model (see text). The linewidth of the individual $5f^n$ final states are set to be equal and multiplet effects are ignored. On the right panel, the energy positions and intensities of the individual $5f^n$ final states are additionally shown by black bars and the f occupancies n_f are given. The insert shows a fit of the experimental data including multiplet effects and energy-dependent lifetime (see the text).

lying final states of mixed-valent compounds of heavy rare earths. For a quantitative analysis of the present data, a least-squares fit was performed based on the sketched SI-Anderson model. The spectral width of the $5f$ states was assumed to scale linear with the distance to the Fermi level by 200-meV per 1 eV binding energy. For both the $5f^1$ and the $5f^2$ state, the corresponding final-state multiplets were adopted. Since for the $4f^1$ emission of γ-like Ce systems the intensity of the $^2F_{5/2}$ emission is considerably larger than the calculated values,[45] the corresponding intensity for the $5f^1$ emission has been taken as a fit parameter in the present study. U_{ff} was assumed to be 3 eV, and δ and Δ were taken as free parameters. Doniach-Sunjic (DS) line shapes superimposed by an integral background were applied to simulate electron-hole-pair creations and other inelastic-scattering events. The simulated spectra were convoluted by a Gaussian of 170 meV to take into account the finite-energy resolution of the experimental setup (150 meV) and thermal broadening ($\sim 4k_BT = 120$ meV). The result of a possible fit with $\Delta = 0.05$ eV and $\delta = 0.10$ eV is shown in the insert of Fig. 8. Contributions of the $5f^0$ state are washed out due to weak intensity and large linewidth (corresponding spectral region is not shown in the insert). At E_F, the linewidth γ of the DS function equals Δ, as it would be expected if interactions with more than one valence-band state were considered. The resulting asymmetry parameter $\alpha \approx 0.3$ is too large as compared to a value $\alpha = 0.1$ expected for d wave screening.[46] The discrepancy might be explained by a nonapplicability of the simple DS approach to the present system or to additional broadening mechanisms such as crystal-field effects that were not considered in our calculation. We have to admit, however, that there are also other weaknesses in the present analysis; the spin-orbit splitting and the $5f_{7/2}/5f_{5/2}$ intensity ratio of the dominating $5f^1$ component have been used as adjustable parameters. This may be justified since the $5f$ occupancy of this state differs from 1, and intensities may change at resonance. To avoid additional fit parameters we have applied the calculated $5f^2$ multiplet[47] without changes, although there the deviations from the atomic configuration are even stronger. One should also note, that the energy of the bare $5f^3$ state might be lower than assumed in Eq. (1) since U_{ff} may depend on the $5f$ occupation. In this case larger $5f^2$ and even $5f^3$ contributions become possible that would affect the line shape. However, as long as no quantitative theoretical predictions for the respective parameters are available, it makes no sense to consider these effects in a numerical simulation.

With our present model calculations we have shown, that a description of the $5f$ spectra within a single-impurity Anderson approach is possible and leads to better results than the application of band-structure calculations. One may argue that the reality lies in between these two extreme positions and should be better described in a periodic Anderson model. Unfortunately such a model is still not available for quantitative calculations of real PE spectra. Since no dispersive $5f$ features are observed in the present experiment we feel no need to go beyond the SI model.

VI. CONCLUSIONS

In summary, a stage-2 U-graphite intercalation compound was *in situ* prepared under UHV conditions by the deposition of U metal onto a (0001) surface of single-crystalline graphite and subsequent annealing. The obtained U-GIC reveals a $(\sqrt{3}\times\sqrt{3})R30°$ reconstruction of the LEED pattern with respect to that of pristine graphite. The samples were studied by means of angle-resolved PE and angle-resolved resonant PE at the $5d \rightarrow 5f$ excitation threshold. The experimental data were compared with results of LDA-LCAO band-structure calculations performed for bandlike and different localized configurations of the $5f$ states. It was shown that the electronic structure of the U-GIC can be understood on the basis of a charge transfer from the U atoms to unoccupied states of graphite. The valence bands are almost tightly shifted toward higher BE's in the intercalation compound. In addition, a rather narrow feature appears at the Fermi energy in the PE spectra of U-GIC that is mainly assigned to a U $5f$ signal that does not reveal multiplet splitting or dispersion. While the shape of the $5f$ emission is not in agreement with the dispersive behavior predicted by band-structure calculation, a description within a simple single-impurity Anderson model is possible.

ACKNOWLEDGMENTS

The authors thank F. von der Decken, Graphitwerk Kropfmühl AG, München, for providing the graphite flakes. This work was supported by the Deutsche Forschungsgemeinschaft Graduiertenkolleg 'Struktur und Korrelationseffekte in Festkörpern' and the Sonderforschungsbereich 463, TP B4 and TP B11, and the Bundesminister für Bildung und Forschung (BMBF), Contract No. 05-SF80D1-4.

*Also at Institute of Physics, St. Petersburg State University, 198904 St. Petersburg, Russia.

[1] S. L. Molodtsov, J. Boysen, M. Richter, P. Segovia, C. Laubschat, S. A. Gorovikov, and A. M. Ionov, Phys. Rev. B **57(20)**, 13 241 (1998).

[2] J. Boysen, P. Segovia, S. L. Molodtsov, W. Schneider, A. Ionov, M. Richter, and C. Laubschat, J. Alloys Compd. **275–277**, 493 (1998).

[3] A. J. Freeman and J. J. B. Darby, *The Actinides: Electronic Structure and Related Properties* (Academic, New York, 1974), Vol. I.

[4] G. R. Stewart, Rev. Mod. Phys. **56(4)**, 755 (1984).

[5] J. E. Fischer and T. E. Thompson, Phys. Today **31**, 36 (1978).

[6] S. Danzenbächer, S. L. Molodtsov, J. Boysen, T. Gantz, C. Laubschat, A. M. Shikin, S. A. Gorovikov, and M. Richter, Physica B **259–261**, 1153 (1999).

[7] S. L. Molodtsov, S. Danzenbächer, M. Richter, and C. Laubschat, Mol. Cryst. Liq. Cryst. **340**, 235 (2000).

[8] S. L. Molodtsov, J. Electron Spectrosc. Relat. Phenom. **96**, 157 (1998).

[9] S. L. Molodtsov, T. Gantz, C. Laubschat, A. G. Viatkine, J. Avila, C. Casado, and M. C. Asensio, Z. Phys. B: Condens. Matter **100**, 381 (1996).

[10] A. M. Shikin, S. L. Molodtsov, C. Laubschat, and G. Kaindl, Phys. Rev. B **51(19)**, 13 586 (1995).

[11] A. Vyatkin, S. Gorovikov, A. Shikin, V. Adamchuk, J. Avila, M. C. Asensio, and S. Molodtsov, Phys. Low-Dimens. Struct. **12**, 339 (1995).

[12] S. L. Molodtsov, C. Laubschat, M. Richter, T. Gantz, and A. M. Shikin, Phys. Rev. B **53**, 16 621 (1996).

[13] A. M. Shikin, G. V. Prudnikova, V. K. Adamchuk, S. L. Molodtsov, T. Gantz, and C. Laubschat, Phys. Low-Dimens. Struct. **7**, 79 (1997).

[14] A. M. Shikin, V. K. Adamchuk, S. Siebentritt, K. H. Rider, S. L. Molodtsov, and C. Laubschat, Phys. Rev. B **61**, 7752 (2000).

[15] A. M. Shikin, S. A. Gorovikov, V. K. Adamchuk, S. L. Molodtsov, P. Engelmann, and C. Laubschat, J. Electron Spectrosc. Relat. Phenom. **105**, 85 (1999).

[16] A. M. Shikin, S. L. Molodtsov, A. G. Vyatkin, V. K. Adamchuk, N. Franco, M. Martin, and M. C. Asensio, Surf. Sci. **429**, 287 (1999).

[17] A. M. Shikin, G. V. Prudnikova, V. K. Adamchuk, S. L. Molodtsov, C. Laubschat, and G. Kaindl, Surf. Sci. **331–333**, 517 (1995).

[18] G. Kaindl, J. Feldhaus, U. Ladewig, and K. H. Frank, Phys. Rev. Lett. **50**, 123 (1983).

[19] M. E. Makrini, D. Guérard, P. Lagrange, and A. Hérold, Physica B **99**, 481 (1980).

[20] L. Hedin and B. I. Lundqvist, J. Phys. C **4**, 2064 (1971).

[21] H. Eschrig, *Optimized LCAO Method* (Springer-Verlag, Berlin, 1989).

[22] M. Richter and H. Eschrig, Solid State Commun. **72**, 263 (1989).

[23] W. Eberhardt, I. T. McGovern, E. W. Plummer, and J. E. Fisher, Phys. Rev. Lett. **44**, 200 (1980).

[24] A. R. Law, J. J. Barry, and H. P. Hughes, Phys. Rev. B **28**, 5332 (1983).

[25] A. Bianconi, S. B. M. Hagström, and R. Z. Bachrach, Phys. Rev. B **16**, 5543 (1977).

[26] E. L. Shirley, L. J. Terminello, A. Santoni, and F. J. Himpsel, Phys. Rev. B **51**, 13 614 (1995).

[27] N. Gunasekara, T. Takahashi, F. Maeda, T. Sagawa, and H. Suematsu, Z. Phys. B: Condens. Matter **70**, 349 (1988).

[28] N. A. W. Holzwarth, S. G. Louie, and S. Rabii, Phys. Rev. B **30**, 2219 (1984).

[29] A. R. Law, M. T. Johnson, and H. P. Hughes, Phys. Rev. B **34**, 4289 (1986).

[30] B. Reihl, N. Mårtensson, and D. E. Eastman, Phys. Rev. B **26**, 1842 (1982).

[31] M. Iwan, E. E. Koch, and F. J. Himpsel, Phys. Rev. B **24**, 613 (1981).

[32] B. Reihl, M. Domke, G. Kaindl, G. Kalkowski, C. Laubschat, F. Hulliger, and W. D. Schneider, Phys. Rev. B **32**, 3530 (1985).

[33] U. Fano, Phys. Rev. **124**, 1866 (1961).

[34] S. L. Molodtsov, M. Richter, S. Danzenbächer, S. Wieling, L. Steinbeck, and C. Laubschat, Phys. Rev. Lett. **78**, 142 (1997).

[35] I. T. McGovern, W. Eberhardt, E. W. Plummer, and J. E. Fischer, Physica B **99**, 415 (1980).

[36] C. Fretigny, D. Marchand, and M. Laguës, Phys. Rev. B **32**, 8462 (1985).

[37] W. Gordy and W. J. O. Thomas, J. Chem. Phys. **24**, 439 (1956).

[38] T. Gouder, C. Colmenares, J. R. Naegele, and J. Verbist, Surf. Sci. **235**, 280 (1989).

[39] A. M. James and M. P. Lord, *Macmillan's Chemical and Physical Data* (Macmillan, London, UK, 1992).

[40] *Table of Periodic Properties of the Elements* (Sargent-Welch Scientific Company, Illinois, 1980).

[41] J. M. Imer and E. Wuilloud, Z. Phys. B: Condens. Matter **66**, 153 (1987).

[42] J. F. Herbst and R. E. Watson, Phys. Rev. Lett. **34**, 1395 (1975).

[43] J. M. Imer, D. Malterre, M. Grioni, P. Weibel, B. Dardel, Y. Baer, and B. Delley, Phys. Rev. B **43**, 1338 (1991).

[44] J. W. Allen, Y. X. Zhang, L. Tjeng, L. E. Cox, M. B. Maple, and C. T. Chen, J. Electron Spectrosc. Relat. Phenom. **78**, 57 (1996).

[45] E. Weschke, A. Höhr, G. Kaindl, S. L. Molodtsov, S. Danzenbächer, M. Richter, and C. Laubschat, Phys. Rev. B **58**, 3682 (1998).

[46] W. D. Schneider and C. Laubschat, Phys. Rev. B **20**, 4416 (1979).

[47] F. Gerken and J. S. May, J. Phys. F: Met. Phys. **13**, 1571 (1983).